A Portable CMOS-based MRI System with 67×67×83 μm³ Image Resolution

Daniel Krüger[1,2], Aoyang Zhang[1], Henry Hinton[1], Victor M. Arnal[1], Yi-Qiao Song[1,4], Yiqiao Tang[4], Ka-Meng Lei[3], Jens Anders[2], and Donhee Ham[1]
[1]Harvard University, Cambridge, MA, USA. [2]University of Stuttgart, Stuttgart, Germany. [3]University of Macau, Macau, China. [4]Schlumberger-Doll Research, Cambridge, MA, USA.
Email: dkrueger@seas.harvard.edu

***Abstract*—This paper presents the smallest-ever, portable CMOS-based magnetic resonance imaging (MRI) system, comprising a fully-integrated and digitally-assisted CMOS RF transceiver IC and a permanent magnet with $B_0 \approx 0.51$ T with the corresponding f_0 for the ^{1}H proton spins being 21.8 MHz. The system has a volume less than a shoebox, weighs less than 10 kg, and provides an imaging volume of 6×6×6 mm³ with an image resolution of 67×67×83 μm³. In addition to MRI, the presented system can also perform multi-dimensional nuclear magnetic resonance (NMR) relaxometry and high-resolution NMR spectroscopy, combining all state-of-the-art NMR modalities in a single, portable device.**

***Keywords*—MRI, NMR, CMOS, imaging, on-chip, portable.**

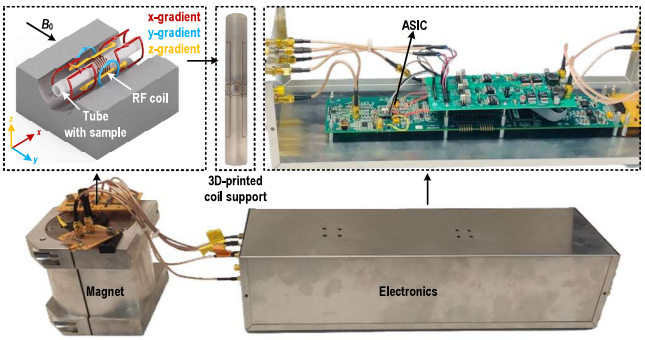

Fig. 1: Portable, CMOS-based MRI system.

I. Introduction

Magnetic Resonance Imaging (MRI) revolutionized medicine with its power to elucidate the tissue structure details and blood flow activities inside the body non-invasively. It is based on nuclear magnetic resonance (NMR), where a nuclear spin (e.g., ^{1}H proton spin) in a static magnetic field (B_0) manifests resonance at an RF frequency of $f_0 = \gamma B_0/2\pi$, with γ being the gyromagnetic ratio of the nuclear spin. An ensemble of nuclear spins in a material (e.g., water or fat) excited by an RF magnetic field at f_0 undergoes precession at f_0, with relaxation times depending on the material composition. MRI is the spatial mapping of local proton densities and relaxation times across the sample, where the mapping is achieved by using magnetic field gradients.

Commercial MRI systems [1], which use superconducting magnets, cryogenic support, and discrete RF electronics are bulky, heavy, costly, and thus available only at dedicated facilities. Their miniaturization into a portable platform–by replacing the superconducting magnet with a permanent magnet and by integrating the RF electronics into a CMOS chip–would enable on-site and on-demand imaging of *ex vivo* biological tissues as well as artificial organoids, small organisms, and organic materials, and can thus further greatly impact medicine and biological/physical sciences all the more. However, while NMR systems without imaging capability have been miniaturized in recent years [2-6], MRI system miniaturization has proven challenging. Although MRI is based on NMR, its miniaturization is more challenging, as it involves a complex engineering due to the additional magnetic field gradients (to choose slices to image) that must work in synchrony with RF magnetic fields (to manipulate the nuclear spins). While a small MRI system was recently reported [7], its magnetic field gradient manipulation, the most essential component of MRI, was not performed on-chip.

Here, we report the smallest-ever portable MRI system consisting of a fully-integrated and digitally-assisted CMOS RF transceiver IC and a 0.51-T permanent magnet (Fig. 1, bottom). With the system occupying a volume of less than 5 liters and weighing less than 10 kg, compared to conventional MRI systems, especially preclinical ones, where samples at the molecular or tissue level (e.g., biopsies) are analyzed, the reported system achieves a volume and weight reduction of 2700 times and 480 times (c.f. [1]), respectively, and provides an imaging volume of 6×6×6 mm³ with an image resolution of 67×67×83 μm³. Moreover, the presented system not only enables MRI, but also multidimensional NMR relaxometry and high-resolution NMR spectroscopy in a single, portable device.

The paper is organized as follows: In Section II we give an overview of the proposed MRI system. Section III describes the utilized NMR transceiver chip architecture with its individual building blocks. In Section IV we discuss the electrical characterization of the chip and provide

measurement results obtained with the presented MRI system. Section V concludes the paper with a brief summary.

II. System Overview

Fig. 1 shows the proposed MRI system. It consists of three main parts, a CMOS integrated RF transceiver circuit, a permanent magnet with $B_0 \sim 0.51\,\mathrm{T}$ with the corresponding f_0 for the ^{1}H proton spins being 21.8 MHz, as well as a set of NMR/MRI and gradient coils. The RF coil, wound around a capillary sample tube, is connected to the CMOS transceiver to inject RF magnetic field pulse sequences that excite the nuclear spins, and to monitor the resulting nuclear spin motions. In addition, the Golay coil pair (red), the Maxwell coil pair (blue), and the Saddle coil pair (yellow) generate the magnetic field gradients necessary for spatial encoding. These three gradient coils are formed around 3D-printed support structures and connected to the field gradient control of the CMOS chip.

Despite the advances in form factor and weight, permanent magnets suffer from lower magnetic field strengths and higher magnetic field inhomogeneities, which significantly lower the MRI signal and therefore impede high resolution MRI. To ameliorate the signal-to-noise (SNR) of the image and realize fast image acquisition, we have designed an application-specific integrated circuit (ASIC), whose die micrograph is shown in Fig. 2.

III. Transceiver ASIC

Fig. 3 shows the block diagram of the CMOS RF transceiver ASIC, highlighting the main building blocks, namely, a low-noise RF receiver, an RF transmitter, a 3D-gradient control, and a digital/mixed-signal controller (pulse programmer digital logic, shift-register memory banks, and delay-locked loop (DLL) based multi-phase generator).

To preserve the already weak MRI signal, it is most important to reduce the receiver noise. Furthermore, to allow for a broad variety of experiments, a large dynamic range is desirable. In order to minimize the SNR degradation and to increase the dynamic range, the front-end of the RF receiver consists of a fully-differential, two-stage, low-noise amplifier (LNA) followed by a digitally controlled (5-bit) attenuator. Further improvement of the receiver noise figure by 3 dB is achieved by using quadrature mixers for frequency down-

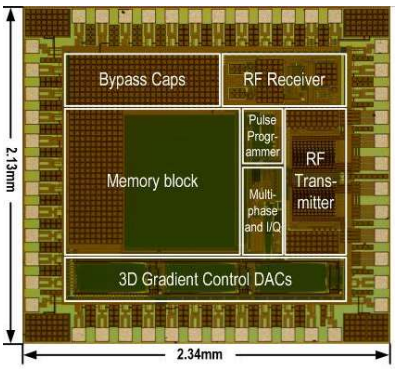

Fig. 2: Annotated micrograph of the transceiver ASIC.

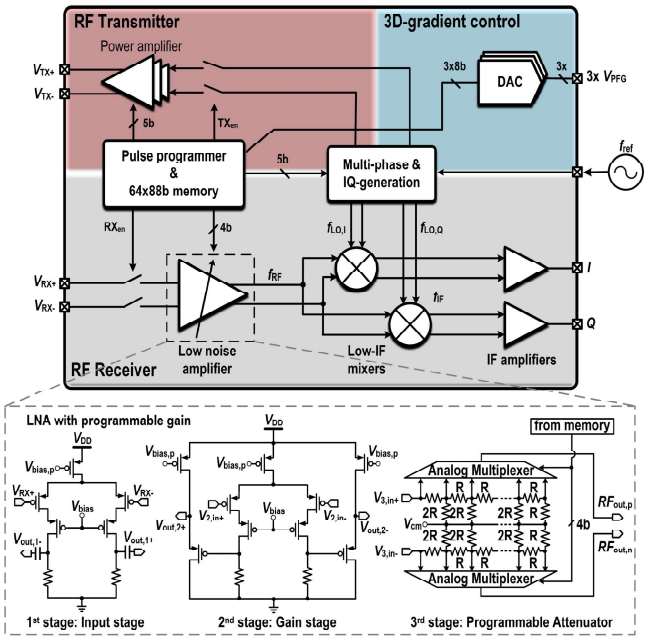

Fig. 3: Block and transistor level diagram of the transceiver ASIC.

conversion. Driven by quadrature local oscillators they produce two intermediate frequency signals, which are subsequently low pass filtered and amplified to produce the two quadrature outputs, I and Q, which jointly contain information on the nuclear spin motion. With an overall, tunable receiver gain of 30 to 100 dB, the receiver dynamic range can be optimally adjusted to the NMR application at hand.

The RF transmitter sends out RF pulse sequences with fine phase and amplitude control in order to manipulate the nuclear spin motion with high precision. The core is a class-D^{-1} power amplifier (Fig. 4, left), which is designed for wide amplitude tuning range, efficiency enhancement, and low AM-AM distortion. It incorporates 32 equally weighted unit amplifiers that run in parallel. Each unit amplifier stacks two NMOS-

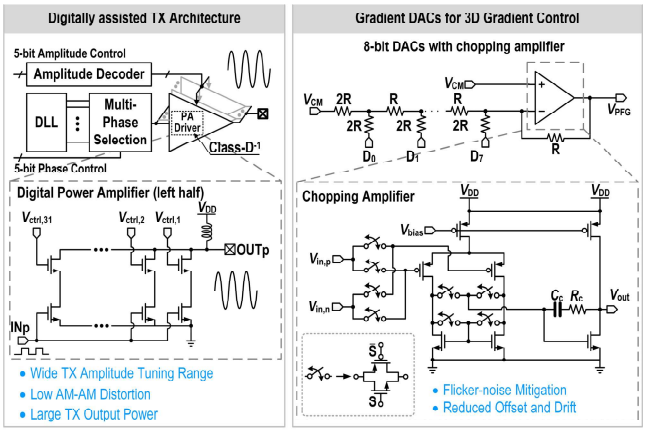

Fig. 4. Block and transistor level diagrams of the digitally assisted transmitter architecture and gradient DACs.

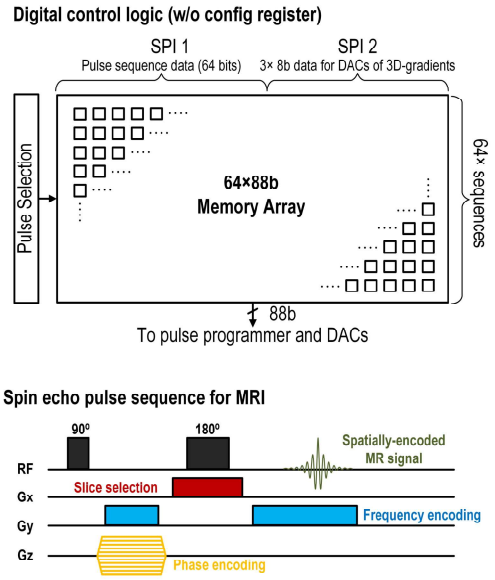

Fig. 5. Digital control logic and utilized MRI sequence.

transistors. The bottom transistor functions as a current source, driven by the phase-modulated RF signal, provided by the on-chip DLL, which produces any one of the 32 different RF phases equally spaced between 0 and 2π, with a phase resolution of $\pi/16$. The cascode transistor acts as a switch, enabled by a 5-bit binary to 31-bit thermometer decoder and controlled by the digital control logic. This enables an RF output amplitude modulation with 31 differing amplitude and 32 phase values, allowing for a broad range of RF pulse sequences.

The most important feature of the presented chip is its 3D-gradient field control (Fig. 4, right), which is essential for MRI. The 3D-gradient control incorporates three 8-bit digital-to-analog converters (DACs) to perform a 3D static magnetic field gradient control in the x, y, and z directions. Each DAC is of the R-2R topology and uses a chopper-stabilized op-amp in a negative feedback loop to mitigate offset, low-frequency drifts and $1/f$ noise for high fidelity. To synchronize relative timings between the field gradients and RF excitation signals, the gradient code for each DAC is stored in the on-chip memory bank, and linked to the corresponding pulse sequence address in the digital control logic (pulse programmer).

This digital control logic, whose simplified function is shown in Fig. 5, manages the entire operation of the chip. It not only controls the phase and amplitude of the RF transmitter (as discussed earlier), but also stores up to 64 sets of digital codes, representing specific pulse sequences, greatly improving the user-friendliness of the presented system. An additional 64-bit configuration register in the memory block is to control common signals and reduces the number of I/O-pads. Setting and refreshing of the memory is done through a standard serial peripheral interface (SPI).

IV. Measurement Results

A. ASIC Characterization

The NMR/MRI transceiver ASIC, fabricated in a standard 0.18 µm CMOS technology, occupies 4.98 mm^2 (Fig. 2). The measured receiver voltage gain ranges from 30 to 100 dB, which by choosing the maximum gain, leads to a measured input-referred voltage noise density at room temperature of 0.78 nV/ √ Hz. The input-referred noise has been obtained by measuring the output voltage noise (differential input shorted) and dividing the results by the previously measured voltage gain.

In addition, we have characterized the RF transmitter. Fig. 6, top left shows the measurement results for the PA. For an output frequency of 21.8 MHz (f_0 = 42.6 MHz · B_0), and a precision 1-Ω load resistor the measured output current of the PA is tunable from 25 mA$_{pp}$ to 290 mA$_{pp}$. With a power-matched load (4.9 Ω), the PA delivers a maximum output power of 220 mW, which certifies an output power tuning range in excess of 14 dB.

Furthermore, for the 3D gradient-control DACs we have measured DNLs less than +/- 0.2 LSB, sufficiently linear for high-resolution imaging (Fig. 6, top left).

B. NMR/MRI Results

Before acquiring the MR images, we first performed NMR spectroscopy (Fig. 6, bottom left) and relaxometry (Fig. 6, top right) experiments.

Fig. 6, bottom left, shows the measured ^{1}H NMR free induction decay (FID) from ethanol, and its corresponding NMR spectrum. Resolving the chemical shifts mandated a static magnetic field resolution better than 1 ppm, which we achieved by utilizing the gradient coils for first-order shimming.

Fig. 6, top right, shows the measured 2D correlations of spin-lattice relaxation time (T_1) and spin-spin relaxation time

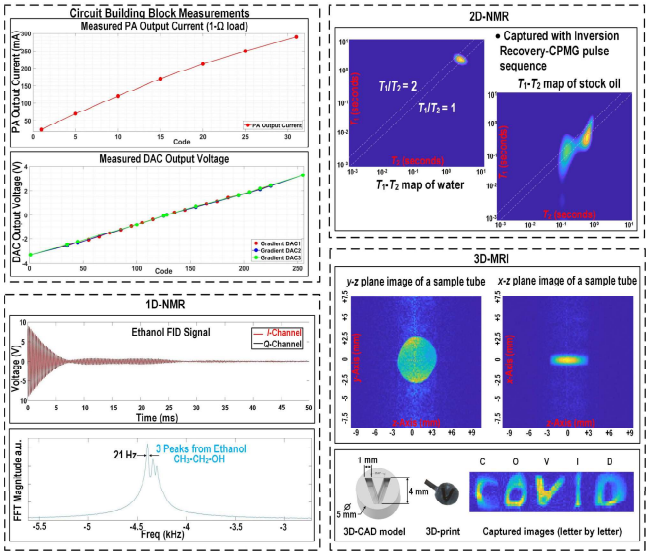

Fig. 6. Measurement results. PA and DAC output, 1D-, and 2D-NMR, as well as 3D-MRI.

TABLE I. Comparison with state-of-the-art.

Specifications	**This work**	[3] H. Bürkle *ESSCIRC'21*	[4] S. Hong *VLSI'20*	[5] K. Lei *ISSCC'16*	[6] N.Sun *ISSCC'10*	[7] K. Lei *Anal. Chem.'20*	[8] J.Handwerker *Nat. Methods'20*
System Performance							
Functionality	**NMR Relaxometry NMR Spectroscopy MRI**	NMR Relaxometry	NMR Relaxometry	NMR Relaxometry	NMR Relaxometry	NMR Relaxometry NMR Spectroscopy MRI	NMR Relaxometry NMR Spectroscopy MRI
Magnet	**Permanent (0.51 T)**	Permanent (1.1 T)	Permanent (0.5 T)	Permanent (0.46 T)	Permanent (0.5 T)	Permanent (0.51 T)	Superconducting (14.1 T)
Imaging	**On-Chip**	N/A	N/A	N/A	N/A	Off-Chip	Off-Chip
ASIC Performance							
Technology	**0.18µm CMOS**	0.35 µm HV-CMOS	0.18 µm CMOS	0.18 µm CMOS	0.18 µm CMOS	0.18 µm CMOS	0.18 µm CMOS
Frequency Range [MHz]	**10-60**	0.1-200	21	20	21	10-40	600
RX IRN [nV/√Hz]	**0.78**	1.1	0.95	N/A	0.93	0.82	1.26
RX Gain [dB]	**30-100**	N/A	65-125	N/A	N/A	34-100	N/A
TX P_{out} [mW]	**220**	500	84	16	80	182	N/A
On-chip AM/PM	**Yes**	No	No	No	Yes	Yes	No
Area (mm^2)	**5**	5.8	1.8	7.6	11.3	4	1.8

(T_2) for water and for stock oil. The more complex T_1-T_2 data for the oil are due to the composition of the coil with various weight hydrocarbon molecules.

For MRI, the three gradient coil pairs are used for slice selection, and phase and frequency encoding, respectively. The Golay coil pair (Fig.1, red coils) generates a field gradient in the *x* direction, the Maxwell coil pair (Fig. 1, blue coils) generates a field gradient in the *y* direction, and the Saddle coil pair (Fig. 1, yellow coils) generates a field gradient along the *z* direction. With the 0 to 3.3 V output voltage range of each DAC, within the magnet bore (diameter: 26 mm), the gradient coils are optimized for a field-of-view of 6 mm, and a field gradient up to 200 mT/m. Fig. 6, bottom right, shows an MRI image of the *y*-*z* cross-section of a tube containing water, and an MRI image of the *x*-*z* cross-section of the same water-filled tube. Furthermore, as also shown in the figure, we have imaged 5 different alphabet phantoms (1 mm deep trenches filled with water) on the *x*-*z* planes. The achieved spatial imaging resolution is as high as 67×67×83 μm^3.

Table I compares this work, the smallest MRI system consisting of a fully-integrated and digitally-assisted CMOS RF transceiver IC, with the recent CMOS-based magnetic resonance systems (mostly limited to NMR [3-6], and the two MRI works using either off-chip gradient control [7] and/or a superconducting magnet [8]).

V. Conclusion

In this paper we have presented the smallest MRI system combining a fully-integrated and digitally-assisted transceiver ASIC and a permanent magnet. For the first time, the gradient control has been implemented on-chip, greatly reducing the complexity of the off-chip electronics and the required programming efforts. In addition to MRI, the system can also perform multi-dimensional NMR relaxometry and high-resolution NMR spectroscopy. Combining all state-of-the-art NMR modalities in a single, portable device, this system presents an important step towards on-site and on-demand imaging of e.g. *ex vivo* biological tissues and can thus further greatly impact medicine and biological/physical sciences.

Acknowledgment

We thank Dr. Isik Kizilyalli, program director of the Advanced Research Projects Agency-Energy (ARPA-E), for the support of this research under contract DE-AR0001063. This work was also funded in part by the University of Macau (MYRG2020-00132-IME).

References

[1] "Ultra high field MRI: BioSpec," *Bruker* [Online]. Available: https://www.bruker.com/en/products-and-solutions/preclinical-imaging/mri/biospec-ultra-high-field-mri.html [Accessed: 4/18/22].

[2] Jens Anders, Frederik Dreyer, Daniel Krüger, Ilai Schwartz, Martin B. Plenio, Fedor Jelezko, "Progress in miniaturization and low-field nuclear magnetic resonance," *Journal of Magnetic Resonance*, Volume 322, 2021.

[3] H. Bürkle, T. Klotz, R. Krapf and J. Anders, "A 0.1 MHz to 200 MHz high-voltage CMOS transceiver for portable NMR systems with a maximum output current of 2.0 App," *ESSCIRC 2021 - IEEE 47th European Solid State Circuits Conference(ESSCIRC)*,2021, pp.327-330.

[4] S. Hong and N. Sun, "A Portable NMR System with 50-kHz IF, 10-us Dead Time, and Frequency Tracking," *2020 IEEE Symposium on VLSI Circuits*, 2020, pp. 1-2.

[5] K.-M. Lei *et al.*, "28.1 A handheld 50pM-sensitivity micro-NMR CMOS platform with B-field stabilization for multi-type biological/chemical assays," *2016 IEEE International Solid-State Circuits Conference (ISSCC)*, 2016, pp. 474-475.

[6] N. Sun *et al.*, "Palm NMR and one-chip NMR," *2010 IEEE International Solid-State Circuits Conference - (ISSCC)*, 2010, pp. 488-489.

[7] K.-M. Lei, Dongwan Ha, Yi-Qiao Song, Robert M. Westervelt, Rui Martins, Pui-In Mak, and Donhee Ham, *Analytical Chemistry 2020* 92 (2), 2112-2120.

[8] Handwerker, J., Pérez-Rodas, M., Beyerlein, M. *et al.* A CMOS NMR needle for probing brain physiology with high spatial and temporal resolution. *Nat Methods* **17,** 64–67 (2020).